Molecular Biology of the Cell
Vol. 5, 29–43, January 1994

Systematic Mutational Analysis of the Yeast β-Tubulin Gene

Renee A. Reijo,* Eric M. Cooper, Gwyneth J. Beagle, and Tim C. Huffaker

Section of Biochemistry and Molecular and Cell Biology, Cornell University, Ithaca, New York 14853

Submitted September 21, 1993; Accepted November 10, 1993
Monitoring Editor: David Botstein

A systematic strategy was used to create a synoptic set of mutations that are distributed throughout the single β-tubulin gene of *Saccharomyces cerevisiae*. Clusters of charged amino acids were targeted for mutagenesis and converted to alanine to maximize alterations on the protein's surface and minimize alterations that affect protein folding. Of the 55 mutations we constructed, three confer dominant-lethality, 11 confer recessive-lethality, 10 confer cold-sensitivity, one confers heat-sensitivity, and 27 confer altered resistance to benomyl. Only 11 alleles give no discernible phenotype. In spite of the fact that β-tubulin is a highly conserved protein, three-fourths of the mutations do not destroy the ability of the protein to support the growth of yeast at 30°C. The lethal substitutions are primarily located in three regions of the protein and presumably identify domains most critical for β-tubulin function. Interestingly, most of the conditional-lethal alleles produce specific defects in spindle assembly at their restrictive temperature; cytoplasmic microtubules are relatively unaffected. The exceptions are two mutants that contain abnormally long cytoplasmic microtubules. Mutants with specific spindle defects were not observed in our previous collection of β-tubulin mutants and should be valuable in dissecting spindle function.

INTRODUCTION

Microtubules are polymers of α- and β-tubulin that are involved in a number of motile processes in eukaryotic cells including intracellular transport of organelles and chromosome separation. The yeast *Saccharomyces cerevisiae* has proven to be a tractable organism to study microtubules. It contains relatively simple microtubule arrays (Peterson and Ris, 1976; Byers, 1981; Kilmartin and Adams, 1984) that participate in a small number of well-defined and readily assayed events (Delgado and Conde, 1984; Huffaker *et al.*, 1988; Jacobs *et al.*, 1988). There is just one structural gene for β-tubulin (*TUB2*) in yeast. It encodes a protein that is 75% identical to animal cell β-tubulins (Neff *et al.*, 1983). This high degree of sequence conservation suggests that the β-tubulin proteins from these cells have retained common biochemical properties. In support of this notion, it has been demonstrated that tubulin from yeast and animal cells will coassemble in vitro (Kilmartin, 1981; Pillus and Solomon, 1986; Barnes *et al.*, 1992). In addition, a chimeric β-tubulin protein that contains both chicken and yeast sequences is incorporated efficiently into all of the microtubule structures of mouse fibroblasts in vivo (Bond *et al.*, 1986). *TUB2* is an essential yeast gene and a number of conditional-lethal alleles have been obtained by a variety of techniques (Thomas *et al.*, 1985; Huffaker *et al.*, 1988; Matsuzaki *et al.*, 1988; Schatz *et al.*, 1988; Stearns and Botstein, 1988). Although these mutations have been useful in defining the major roles of microtubules in yeast, they do not display the complete range of phenotypes that could be anticipated. In addition, all of the mutations that have been sequenced reside in the C-terminal half of the protein. Thus, it is likely that these mutations identify only a minor fraction of the functional domains of β-tubulin. We reasoned that a more systematic mutagenesis approach would be needed to create a synoptic set of mutations in this gene.

"Clustered charged-to-alanine scanning mutagenesis" has proven to be particularly effective in systematically studying surface domains of proteins (Bass *et al.*, 1991; Bennett *et al.*, 1991; Gibbs and Zoller, 1991).

* Present address: Whitehead Institute, 9 Cambridge Center, Cambridge, MA 02142.

In this approach a protein's primary sequence is scanned for clusters of charged amino acids and each charged residue in the group is converted to alanine. This method exploits the fact that clusters of charged amino acids are likely to occupy exposed positions on the protein. By targeting these residues for mutagenesis, one reduces the number of mutations that affect protein folding. In addition, one enriches for alterations of residues that are likely to be involved in protein-protein interactions. Wild-type charged residues are replaced with alanine because its side group is small and uncharged and thus unlikely to impose severe constraints on secondary structure and tertiary conformation. In this way, a relatively few alleles are needed to survey a significant portion of a protein's surface in an unbiased manner. This approach was recently used to create 34 mutations in the yeast actin gene (Wertman *et al.*, 1992).

In this paper we present a clustered charged-to-alanine scan of yeast β-tubulin. We have assessed the effect of each mutation on β-tubulin function by examining the phenotype of cells carrying the altered allele.

MATERIALS AND METHODS

Yeast Strains and Media

Yeast strains YPH102 (*MATα ura3-52 lys2-801 ade2-101 leu2-Δ1 his3-Δ200*) and YPH250 (*MATa ura3-52 lys2-801 ade2-101 leu2-Δ1 his3-Δ200 trp1-Δ1*) (Sikorski and Hieter, 1989) were obtained from P. Hieter (Johns Hopkins Medical School, Baltimore, MD). Yeast media are described by Sherman (1991). All yeast and bacterial transformations were by electroporation (Becker and Guarente, 1991; Sheen, 1991).

Plasmid Constructions

The plasmid pRR190 (diagrammed in Figure 2) was used to introduce mutations into the *TUB2* gene. Construction of this plasmid required several steps. pTH17 contains the *TUB2* gene on 5.5 kilobase (kb) of yeast genomic DNA. The *Sal* I fragment of pTH17, which includes the C-terminal 65 nucleotides of *TUB2* coding sequence and ~1240 basepairs (bp) of downstream noncoding sequence, was cloned into the *Sal* I site of pRS316 (Sikorski and Hieter, 1989) to create pRR163. It contains a single *Bgl* II site located 840 bp downstream of the *TUB2* coding sequence. An 1170-bp *Bgl* II fragment from pMA1021 containing *URA3* was ligated into the *Bgl* II site of pRR163 to create pRR168. The *Sal* I fragment of pTH17 was then replaced with the *Sal* I fragment of pRR168 to create pRR170. pRR183 is pBluescript II-KS$^+$ (Stratagene, La Jolla, CA) with the *Sma* I site in the polylinker converted to an *Sph* I site. The 4-kb *Nar* I to *Sph* I fragment from pRR170 was cloned into the *Sph* I site of pRR183 using *Sph* I linkers to yield pRR190. Thus, pRR190 contains the entire *TUB2* gene with about 200 bp upstream and 1240 bp downstream of the coding sequence, and *URA3* inserted 840 bp downstream of *TUB2*. This sequence can be removed from pRR190 as a single linear DNA fragment by digestion with *Sph* I.

pRR152 contains a *LEU2*-marked *tub2* deletion allele (*tub2-Δ1::LEU2*). It was constructed by digesting pJT71, which contains *TUB2* including 400 bp upstream and 1240 bp downstream of the coding sequence (Thomas *et al.*, 1985), with *Bgl* II and ligating to a *LEU2* containing *Bam*H I fragment from pRR151. In pRR152, *LEU2* replaces *TUB2* from 85 bp upstream to 840 bp downstream of the coding sequence.

pKFW46 contains the *ACT1* locus with *HIS3* inserted into genomic sequences downstream of *ACT1* (Wertman *et al.*, 1992).

Oligonucleotide-directed Mutagenesis

Oligonucleotide-directed mutagenesis was performed using the MutaGene kit (BioRad, Richmond, CA). Oligonucleotides were designed to contain ≥12 and 9 nucleotides of perfect homology on the 5′ and 3′ sides, respectively, of the mutant sites. Single-stranded DNA containing the anti-sense strand of *TUB2* was produced by transforming pRR190 into CJ236 cells (*dut-1, ung-1, thi-1, rel-1-A*, pCJ105 [Cm^r]) and superinfecting with the helper phage M13K07. Phosphorylated oligonucleotides (15 pmol) were annealed to the single-stranded DNA (~0.1 μg) and used to prime synthesis of the second strand. Plasmids were recovered after transformation into MV1190 cells (Δ(lac-proAB), thi, sup E, (Δsr1-recA)306::Tn10(tet^r) [F′:traΔ36, proAB, lac IqZΔM15]). Mutant plasmids were identified by restriction digestion or double-stranded sequencing (Sequenase system, United States Biochemical, Cleveland, OH).

Construction of the Recipient Diploid Yeast Strain

The recipient diploid yeast strain CUY409 was constructed as follows. YPH102 was transformed with the *ACT1::HIS3* containing *Eco*RI fragment of pKFW46 to produce RRY222. This places *HIS3* on chromosome VI downstream of *ACT1* that is closely linked to *TUB2*. RRY222 was crossed to YPH250, and the diploid was sporulated. Because the *trp1-Δ1* allele confers cold-sensitivity, one Trp$^+$His$^+$ haploid segregant (CUY408) was mated to YPH102. This diploid was transformed with the *tub2-Δ1::LEU2* containing *Sca* I to *Sph* I fragment of pRR152 to disrupt one of the genomic copies of *TUB2*. One transformant, CUY409, was sporulated. As expected, no viable Leu$^+$ spores were recovered because the *TUB2* gene is essential. Tetrads contained only two viable spores that were His$^+$Leu$^-$. Thus, the *tub2* disruption occurred on the copy of chromosome VI that was not marked with *HIS3* as desired.

Allele Replacement in Yeast

Plasmids containing the desired mutations were digested with *Sph* I and transformed into CUY409 cells. Ura$^+$ transformants were selected, and Leu$^-$ transformants were then identified by replica plating. Ura$^+$Leu$^-$ diploids were sporulated, and tetrads were analyzed. The presence of the mutations in yeast was verified by DNA sequence analysis of haploid segregants if they were viable. Polymerase chain reaction (PCR) was used to amplify a 1.8-kb genomic DNA fragment containing the *TUB2* gene. The upstream primer was 5′-GAATTCCCGATCAACAGCAGTTTGAACAGG-3′; the downstream primer was 5′-ACCGTACTGCAGAAGTGCTTCAATCCTAG-3′. The PCR product was ethanol precipitated and digested with a diagnostic restriction enzyme (see Table 1). For those mutations that did not confer a diagnostic restriction site, the PCR product was gel purified and sequenced using a primer ~100 bp upstream of the mutation. For the recessive-lethal alleles, DNA sequence analysis was used to confirm the presence of the expected *tub2* mutations in the heterozygous diploids. PCR was used to amplify genomic DNA fragments from the transformed diploid. This generated two fragments; one contained the wild-type and one contained the mutant *tub2* gene. Presence of the mutant allele was determined by the appearance of a diagnostic restriction fragment (see Table 1). The phenotypes of 22 of the 25 dominant-, recessive-, and conditional-lethal mutations, as well as six of the 30 additional mutations, were further verified by integration of a second, independent clone into yeast. This was not done for the recessive-lethal alleles *tub2-415* and *tub2-425* and the dominant-lethal allele *tub2-453* because only one independent mutant clone was isolated. In all cases, independent clones produced the same phenotype in yeast.

Analysis of Recessive-Lethal Alleles

Heterozygous diploids containing recessive-lethal *tub2* alleles were sporulated in SPM medium (Kassir and Simchen, 1991), and random spores were isolated (Treco and Winston, 1991). Spores were then

plated directly after germination in YPD at 30°C for 4 and 12 h. Plating conditions included YPD at 14, 30, and 37°C; YPD containing 10, 20, 30, 40, 50, or 60 μg/ml benomyl at 30°C; and YPD containing 1 M sorbitol, 1 M KCl, or 0.5 M KCl at 30°C. Colonies were replica plated to determine whether they were Ura^+His^+ (residual diploids), Ura^-His^+ (*TUB2*$^+$ haploids), or Ura^+His^- (*tub2*$^-$ haploids).

For immunofluorescence, random spores were incubated in YPD at 30°C for 7 h. Cells were then fixed and processed for immunofluorescence. Large-budded cells were identified by Nomarski optics and then scored for DNA and microtubule staining.

Fluorescence Staining of Cells

DNA staining with 4′,6′-diamidino-2-phenylindole (DAPI) and microtubule staining by immunofluorescence were performed as described previously (Sullivan and Huffaker, 1992).

RESULTS

Design of Mutations

The charged amino acids (Arg, Asp, Glu, and Lys) of β-tubulin were systematically mutated to alanine by oligonucleotide-directed mutagenesis. To limit the number of mutations needed to cover the entire protein, up to three charged residues were mutated together when they were clustered within a short segment of amino acids. For all but three of the mutations, this segment was up to five amino acids. In the other three mutations, the charged residues spanned seven (*tub2-438* and *tub2-453*) and ten amino acids (*tub2-409*). In one mutation (*tub2-451*), we did not change one of the charged residues of the cluster because a mutation (*tub2-405*) that alters this residue alone has been characterized previously (Huffaker *et al.*, 1988). Altogether, 49 mutations comprising 91 charged-to-alanine changes were constructed. Their positions are diagrammed in Figure 1. Seven charged residues that do not reside in charged clusters were not altered in any of the mutations.

We also constructed six mutations that do not contain solely charged-to-alanine changes. It has recently been reported (Barnes *et al.*, 1992) that the original published sequence of the TUB2 gene (Neff *et al.*, 1983) contains three errors in codons 9, 12, and 159, respectively. During the course of this work, we discovered three additional errors. Codon 71 is GGG (Gly), not TGG (Trp); codon 152 is ATC (Ile), not TTC (Phe); codon 156 is AGG (Arg), not AAG (Lys). Significantly, the amino acids encoded at each of these three positions are now predicted to be identical to those in most animal cell β-tubulins. Initially, oligonucleotides that spanned these three regions of the gene were designed using the published sequence. Thus, they included point mutations in addition to the desired charged-to-alanine mutations. *tub2-414* and *tub2-415* contain the G71W mutation, *tub2-423* contains the I152F mutation, *tub2-426* contains the R156K mutation, and *tub2-424* contains both the I152F and R156K mutations. Mutations containing only the desired charged-to-alanine changes were subsequently made and included in the 49 mutations described above. Finally, in one mutation (*tub2-431*) we made a histidine-to-alanine change. All mutations are listed in Table 1.

To simplify identification of the mutant alleles, we tried to design each mutation so that it produced either a gain or loss of a restriction enzyme site. To accomplish this goal, we used all four alanine codons in designing the set of mutations (see Table 1). However, we did not make silent changes in any of the other codons. All but five of the mutations could be verified by restriction digests; the other five required DNA sequencing. GCA and GCG are relatively minor alanine codons in yeast (Guthrie and Abelson, 1982), but we did not anticipate any problem with using them. The wild-type *TUB2* gene contains both, one GCG and six GCA codons. Our results also indicate that inclusion of these codons does not affect β-tubulin production. Six of the 11 mutations that confer no noticeable phenotype in yeast introduced one or more of these two codons.

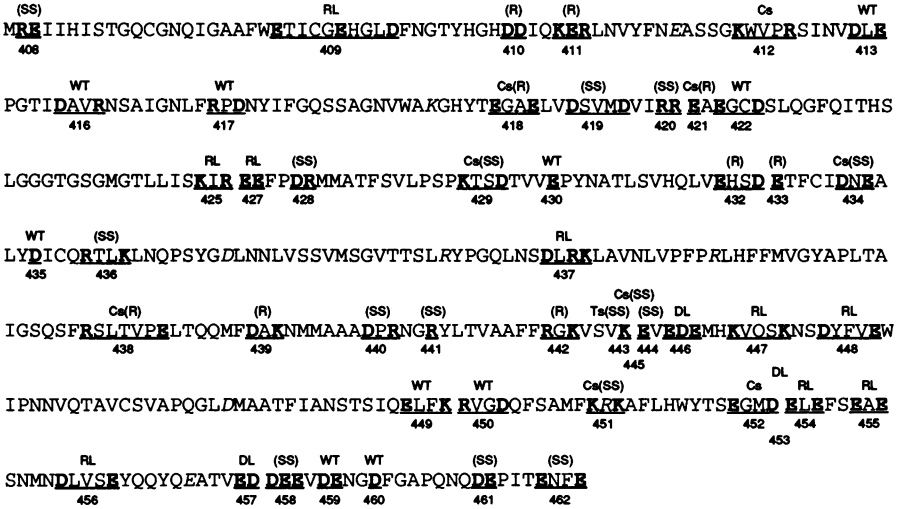

Figure 1. Positions of charged-to-alanine substitutions. The single-letter code for the amino acid sequence of yeast β-tubulin is shown. The charged clusters that were altered are underlined, and residues that were replaced with alanine are in bold letters. The allele number of each mutation is indicated below the sequence. The phenotype of each mutation is indicated above the sequence. Charged residues that were not altered in any of the mutations are in italics. WT, wild-type; DL, dominant-lethal; RL, recessive-lethal; Cs, cold-sensitive; Ts, heat-sensitive; (R), benomyl resistant; (SS), benomyl supersensitive.

Table 1. Summary of mutations

Allele	Amino acid replacement	Codon replacement	Detection[a]	Phenotype[b]
tub2-408	R2A, E3A	AGA2GCT, GAA3GCT	*Xmn* I (−)	BenSS
tub2-409	E22A, E27A, D31A	GAA22GCT, GAG27GCA, GAT31GCT	*Apa*L I (+)	RL
tub2-410	D40A, D41A	GAC40GCT, GAT41GCT	*Eco*R V (−)	BenR
tub2-411	K44A, E45A, R46A	AAG44GCG, GAG45GCC, AGA46GCA	*Not* I (+)	BenR
tub2-412	K58A, R62A	AAG58GCT, AGA62GCT	*Bgl* II (−)	Cs
tub2-413	D67A, E69A	GAT67GCT, GAA69GCT	*Taq* I (−)	WT
tub2-414	D67A, E69A, G71W	GAT67GCT, GAA69GCT, GGG71TGG	*Taq* I (−)	WT
tub2-415	G71W, D74A, R77A	GGG71TGG, GAC74GCT, CGC77GCT	*Pst* I (+)	RL
tub2-416	D74A, R77A	GAC74GCT, CGC77GCT	*Pst* I (+)	WT
tub2-417	R86A, D88A	AGA86GCA, GAC88GCA	*Bsp*M I (+)	WT
tub2-418	E108A, E111A	GAA108GCT, GAG111GCT	*Pvu* II (+)	Cs, BenR
tub2-419	D114A, D118A	GAC114GCT, GAT118GCT	*Nhe* I (+)	BenSS
tub2-420	R121A, R122A	AGA121GCA, CGA122GCT	*Fnu*4H I (+)	BenSS
tub2-421	E123A	GAG123GCT	*Fnu*4H I (+)	Cs, BenR
tub2-422	E125A, D128A	GAA125GCA, GAC128GCA	*Fsp* I (+)	WT
tub2-423	I152F, K154A, R156A	ATC152TTC, AAG154GCC, AGG156GCT	*Taq* I (−)	Cs
tub2-424	I152F, R156K, E157A, E158A	ATC152TTC, AGG156AAG GAA157GCT GAG158GCT	*Xmn* I (−)	RL
tub2-425	K154A, R156A	AAG154GCC, AGG156GCT	*Taq* I (−)	RL
tub2-426	R156K, E157A	AGG156AAG, GAA157GCT	*Xmn* I (−)	BenSS
tub2-427	E157A, E158A	GAA157GCT, GAG158GCT	*Xmn* I (−)	RL
tub2-428	D161A, R162A	GAT161GCA, CGT162GCA	*Pst* I (+)	BenSS
tub2-429	K174A, D177A	AAG174GCC, GAC177GCC	*Msp* I (+)	Cs, BenSS
tub2-430	E181A	GAA181GCG	*Bst*U I (+)	WT
tub2-431	E194A, H195A, E198A	GAA194GCA, CAC195GCA, GAA198GCA	*Alw*N I (+)	BenR
tub2-432	E194A, D197A	GAA194GCA, GAT197GCA	*Pst* I (+)	BenR
tub2-433	E198A	GAA198GCA	*Sfa*N I (+)	BenR
tub2-434	D203A, E205A	GAT203GCG, GAA205GCT	*Cla* I (−)	Cs, BenSS
tub2-435	D209A	GAC209GCT	Sequence	WT
tub2-436	R213A, K216A	AGG213GCA, AAG216GCT	*Ava* II (−)	BenSS
tub2-437	D249A, R251A, K252A	GAT249GCC, AGA251GCC, AAG252GCC	*Fnu*4H I (+)	RL
tub2-438	R282A, E288A	AGA282GCT, GAA288GCT	*Bgl* II (−)	Cs, BenR
tub2-439	D295A, K297A	GAT295GCG, AAG297GCT	*Not* I (+)	BenR
tub2-440	D304A, R306A	GAT304GCG, AGA306GCT	*Bst*U 1 (+)	BenSS
tub2-441	R309A	AGA309GCG	Sequence	BenSS
tub2-442	R318A, K320A	AGA318GCA, AAA320GCA	*Bsp*M I (+)	BenR
tub2-443	K324A	AAG324GCA	*Mse* I (−)	Ts, BenSS
tub2-444	E325A	GAG325GCT	Sequence	BenSS
tub2-445	K324A, E325A	AAG324GCA, GAG325GCT	*Pvu* II (+)	Cs, BenSS
tub2-446	E327A, D328A, E329A	GAA327GCT, GAT328GCA, GAA329GCT	*Pst* I (+)	DL
tub2-447	K332A, K336A	AAA332GCT, AAA336GCT	*Sph* I (+)	RL
tub2-448	D339A, E343A	GAC339GCT, GAA343GCC	*Bst*N I (+)	RL
tub2-449	E376A, K379A	GAG376GCA, AAG379GCG	*Nru* I (+)	WT
tub2-450	R380A, D383A	AGA380GCA, GAC383GCA	*Apa*L I (+)	WT
tub2-451	K390A, K392A	AAA390GCT, AAA392GCT	*Hind* III (−)	Cs, BenSS
tub2-452	E401A, D404A	GAA401GCT, GAC404GCT	Sequence	Cs
tub2-453	E401A, D404A, E407A	GAA401GCT, GAC404GCT, GAA407GCT	*Eco*R I (−)	DL
tub2-454	E405A, E407A	GAA405GCT, GAA407GCT	*Eco*R I (−)	RL
tub2-455	E410A, E412A	GAG410GCA, GAA412GCA	*Pst* I (+)	RL
tub2-456	D417A, E421A	GAT417GCC, GAA421GCG	*Bst*N I (+)	RL
tub2-457	E431A, D432A	GAA431GCT, GAT432GCA	*Pst* I (+)	DL
tub2-458	D433A, E434A, E435A	GAT433GCT, GAA434GCT, GAA435GCT	*Fnu*4H I (+)	BenSS
tub2-459	D437A, E438A	GAC437GCT, GAA438GCT	*Sal* I (−)	WT
tub2-460	D441A	GAT441GCG	*Bst*U I (+)	WT
tub2-461	D449A, E450A	GAT449GCG, GAA450GCG	*Nar* I (+)	BenSS
tub2-462	E454A, E457A	GAG454GCA, GAA457GCA	Sequence	BenSS

[a] Restriction enzyme site either created (+) or destroyed (−) in the mutant allele; sequence indicates that no sites are changed.

[b] WT, wild-type; DL, dominant-lethal; RL, recessive-lethal; Cs, cold-sensitive; Ts, heat-sensitive; BenR, benomyl resistant; BenSS, benomyl supersensitive.

Insertion of Mutations into Yeast

The plasmid used for mutagenesis (pRR190) contains the entire *TUB2* gene on a 2.7-kb genomic DNA fragment. The *URA3* gene is inserted into this fragment at a *Bgl* II site downstream of the *TUB2* coding region. After mutagenesis, the *TUB2::URA3* linear DNA fragment was released from the plasmid by restriction enzyme digestion and transformed into a recipient diploid strain. In the recipient diploid (CUY409), one copy of chromosome VI contains the *HIS3* gene inserted just downstream of *ACT1*, which is tightly linked to *TUB2*. In the other copy of chromosome VI, *LEU2* replaces the *TUB2* coding region and upstream and downstream sequences defined by two *Bgl* II sites. The desired transformant was one in which the mutated copy of *TUB2* integrated into the latter copy of chromosome VI and replaced *LEU2*. Because the transforming fragment has homology to this chromosome only at its ends, integration must introduce the entire *TUB2* coding region, and hence the mutation, and the *URA3* gene. Such transformants were obtained by selecting for *URA3* and screening for loss of *LEU2*. This scheme is diagrammed in Figure 2.

When CUY409 was transformed with the unmutagenized *TUB2::URA3* fragment from pRR190, ~5% of the Ura^+ transformants were also Leu^-. The relatively low frequency of integration into the *LEU2* marked copy of chromosome VI was expected. Most integration events occur on the other copy of chromosome VI because the transforming fragment has significantly more sequence homology to the intact *TUB2* locus. Individual Ura^+Leu^- transformants were sporulated and dissected. Tetrads yielded two Ura^+His^- and two Ura^-His^+ spores. The haploid segregants were uniformly healthy and did not display any altered sensitivity to high or low temperatures or benomyl.

After integration of mutant alleles into CUY409, Ura^+Leu^- diploids were sporulated, and tetrads were dissected. For 41 of the 52 mutations recovered, tetrads produced four viable spores (2:2, Ura^+His^-:Ura^-His^+) indicating that the mutant *tub2* allele can support cell growth at 30°C. Segregants were assayed for growth over a broad range of temperatures (12–37°C) and in the presence of various concentrations of benomyl (0–80 μg/ml) at 30°C. Altered sensitivity to temperature or benomyl, when observed, always segregated 2:2 and was found only in the Ura^+His^- segregants. Thus, all novel phenotypes were linked to the mutant *tub2* alleles. The presence of the expected *tub2* mutations was confirmed by DNA sequence analysis of haploid segregants (see MATERIALS AND METHODS).

Eleven of the 52 recovered mutations resulted in a recessive-lethal phenotype. Tetrads produced only two viable spores; these were always Ura^-His^+ demonstrating linkage of lethality to the *tub2* allele. DNA sequence analysis confirmed the presence of the expected *tub2* mutations in the heterozygous diploids (see MATERIALS AND METHODS). These results only indicate that the recessive-lethal mutants cannot grow under our standard spore germination conditions (YPD at 30°C). We investigated whether some of these mutants fail to grow on YPD at 30°C because they are extremely heat-sensitive (Ts) or cold-sensitive (Cs), because they require benomyl for growth (benomyl-dependence has been observed for *tub2* alleles [Thomas *et al.*, 1985]), or because they require osmotic support. Using random spore

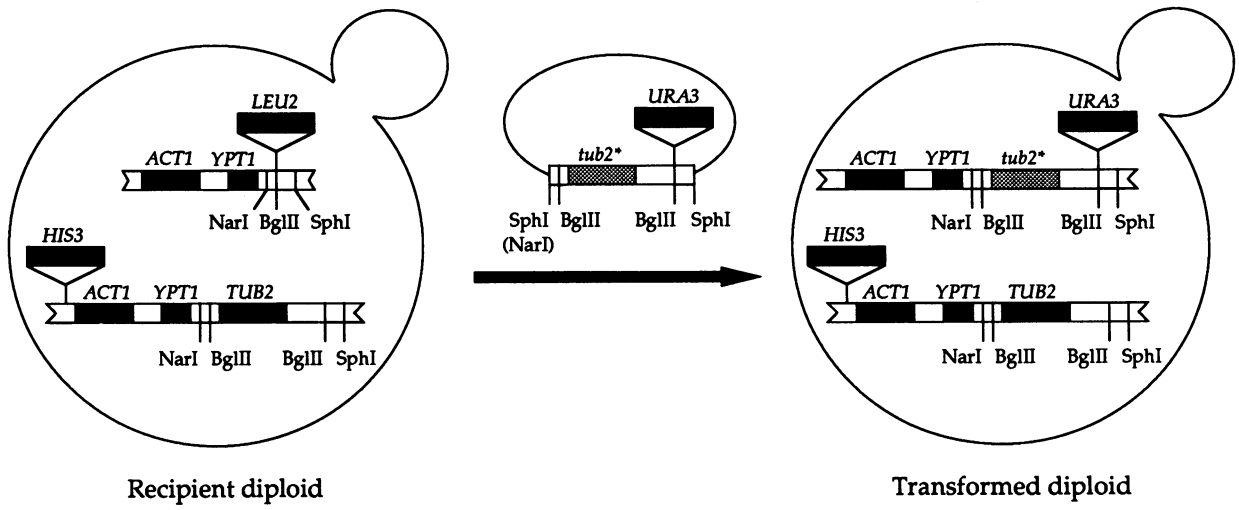

Figure 2. Construction of diploid yeast strains containing mutant *tub2* allele. A mutant allele of *TUB2* (*tub2**) was made in plasmid pRR190 by oligonucleotide-directed mutagenesis. The recipient diploid strain was transformed with the *Sph* I fragment of this plasmid. Transformants were selected for gain of *URA3* and screened for loss of *LEU2* to obtain cells in which the mutant allele replaced the *LEU2* disrupted copy of *TUB2*. Sporulation of the transformed diploid yielded haploids containing the mutant *tub2* allele. When viable, these were Ura^+ and His^-.

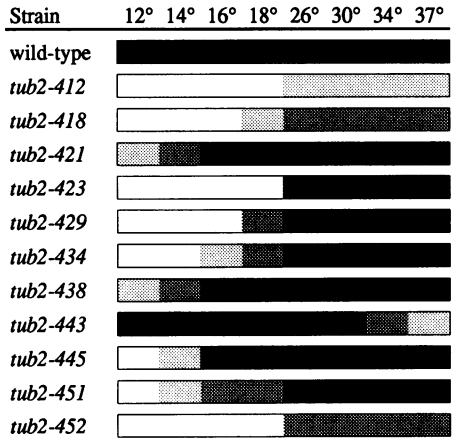

Figure 3. Growth of wild-type and mutant strains. Growth at each temperature was scored on YPD plates and is relative to growth of the wild-type strain at the same temperature. Growth is proportional to stippling: wild-type growth = heavy stippling > medium stippling > light stippling > no stippling = no growth.

analysis, we screened for growth at different temperatures (14, 30, and 37°C), at different benomyl concentrations (10–60 μg/ml), and with osmotic support (1 M sorbitol, 0.5 and 1 M KCl). None of these conditions allowed growth of any of the 11 recessive-lethal mutants.

We were unable to recover transformants containing three of the alleles we constructed. When these mutations were transformed into yeast, the frequency of Leu^- isolates among the Ura^+ transformants was reduced about 10-fold relative to the results obtained with all other alleles. Tetrad analysis of these Ura^+Leu^- diploids revealed that the transformants had become homozygous at the flanking *ACT1* locus (4:0, His^+:His^-). This latter result indicates the participation of the intact *TUB2* locus in the event that replaced *tub2-Δ1::LEU2*. Thus, the *tub2-446*, *tub2-453*, and *tub2-457* alleles most likely cause dominant-lethality.

Phenotypic Characterization of the Viable Mutants

Ten of the mutant alleles are Cs, and one is Ts for growth. The permissive temperature ranges for the Cs mutants vary considerably (Figure 3). For example, *tub2-423* cells fail to grow at 18°C; *tub2-421* and *tub2-438* cells grow weakly even at 12°C. Most of the Cs mutants grow as well as wild-type cells at all temperatures above 26°C. The exceptions are *tub2-412*, *tub2-418*, and *tub2-452* cells that grow more slowly at these temperatures. The Ts mutant *tub2-443* grows well at ≤30°C and weakly at 37°C. All of the Cs and Ts alleles are recessive; heterozygous diploids containing one wild-type and one mutant *tub2* allele grow as well as wild-type diploids at all temperatures.

Many of the *tub2* mutants display altered sensitivity to benomyl. Wild-type haploid cells grow well on 20 μg/ml of benomyl but fail to grow on 30 μg/ml. Seventeen of the mutants are more sensitive, and 10 are more resistant to benomyl than wild-type cells. The degree of sensitivity and resistance varies (Figure 4). Five mutants fail to grow or grow only poorly on 5 μg/ml benomyl, the lowest concentration tested; five mutants grow on 80 μg/ml benomyl, the highest concentration tested.

Cell Cycle Arrest of Cs and Ts Mutants

Mutations or drug treatments that eliminate all cellular microtubules cause yeast cells to arrest with a uniform terminal morphology (Huffaker *et al.*, 1988; Jacobs *et al.*, 1988). Arrested cells possess a large bud and a single undivided nucleus randomly located within the mother

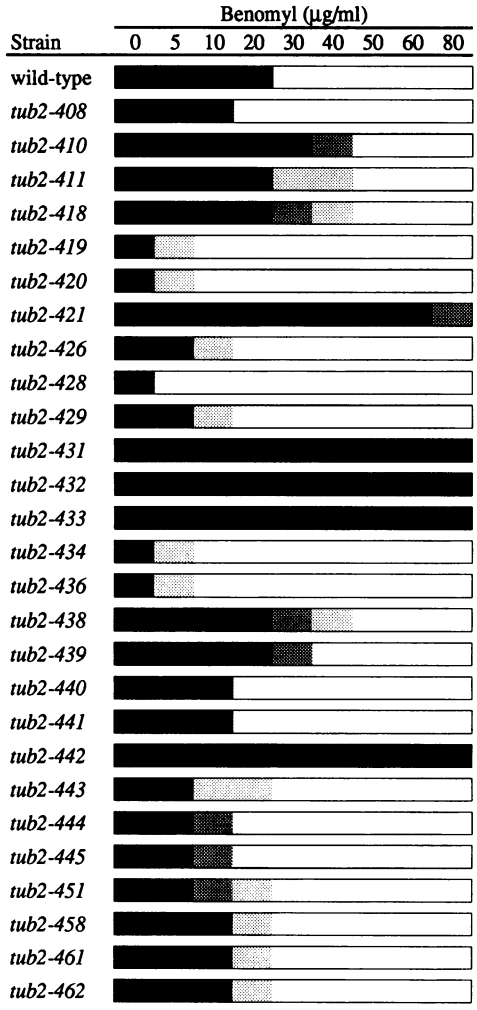

Figure 4. Growth of wild-type and mutant haploid strains on benomyl. Growth on YPD plus benomyl was scored at 30°C and is relative to growth of the wild-type on YPD without benomyl. Growth is proportional to stippling: heavy stippling > medium stippling > light stippling > no stippling = no growth.

cell. This phenotype indicates that microtubules are required for both migration of the nucleus to the bud neck and subsequent nuclear division. Cytoplasmic microtubules are responsible for nuclear migration but are not required for nuclear division (Huffaker *et al.*, 1988; Sullivan and Huffaker, 1992). A mutation that interferes only with nuclear microtubule function will block nuclear division but not migration and cause cells to arrest with an undivided nucleus located at the bud neck. Conversely, if only cytoplasmic microtubule function is affected, nuclear division will take place in the absence of nuclear migration and produce binucleate cells with two nuclei in one cell body.

To determine whether the new *tub2* mutants exhibit a uniform arrest phenotype, we shifted asynchronous cultures to their restrictive temperatures for two generation times. We used 12°C as the restrictive temperature for most of the Cs mutants. For *tub2-423*, which is extremely Cs, we used 14°C. The restrictive temperature for the Ts mutant *tub2-443* was 37°C. In all of the *tub2* mutant cultures, large-budded cells accumulate at the restrictive temperature (Figure 5A). The extent of the accumulation is roughly proportional to the degree of cold sensitivity or heat sensitivity. As expected, those mutants that grow weakly even at the most restrictive temperatures display only modest cell cycle arrests. The nuclear DNA in large-budded cells was visualized by DAPI staining. Most wild-type large-budded cells have completed chromosome separation and contain a DAPI-staining region in both the mother and bud cell bodies. For all but one mutant, >70% of the large bud-arrested cells contain a single staining region (Figure 5B). Only in the *tub2-421* culture do a majority of cells have divided nuclei (56%). Thus, all but one of the mutations produce a significant block of nuclear division.

For cells that contained an undivided nucleus, we scored the fraction in which the nucleus had migrated to the bud neck. Nuclear migration was said to occur if any portion of the DAPI staining extended up to or through the bud neck. Interestingly, in none of the mutants is the undivided nucleus randomly located in the mother cell. Nuclear migration occurs in ~60–90% of the cells depending on the *tub2* allele. These results can be compared to our previous results with *tub2-401* cells that lack all microtubules at 12°C (Huffaker *et al.*, 1988). Only 15% of *tub2-401* cells contain a DAPI-staining region adjacent to the bud neck; we attribute these to random distribution of nuclei in the mother cells. Thus, all of the new mutants retain the capacity for nuclear migration. In a few mutants nuclear migration is slightly less efficient indicating a partial inhibition of cytoplasmic microtubule function.

Microtubule Assembly in Cs and Ts Mutants

Unbudded wild-type cells contain a single spindle pole body (SPB), the microtubule organizing center in yeast,

Strain	Temp.	A			B			
wild-type	12°	43	45	12	0	9	91	0
tub2-412	12°	8	9	83	35	56	8	1
tub2-418	12°	10	9	81	29	60	8	3
tub2-421	12°	17	32	51	12	32	42	14
tub2-423	14°	9	1	90	33	67	0	0
tub2-429	12°	4	14	82	10	87	3	0
tub2-434	12°	8	12	80	12	81	7	0
tub2-438	12°	29	25	46	6	68	24	2
tub2-443	37°	15	21	64	30	53	13	4
tub2-445	12°	15	12	73	15	74	9	2
tub2-451	12°	9	15	76	14	80	5	1
tub2-452	12°	12	23	65	27	45	23	5

Figure 5. Cell and nuclear morphologies. Cells were grown at 30°C, shifted to the indicated restrictive temperature for two generation times, and stained with DAPI. (A) The percentages of cells that were unbudded, small-budded, or large-budded are indicated. A large-budded cell possesses a bud whose diameter is at least three-fourths the diameter of the mother cell. (B) The percentages of large-budded cells that possessed a particular nuclear morphology are indicated. Four types of nuclear morphology were scored: an undivided nucleus in one cell body, an undivided nucleus at the bud neck, divided nuclei properly segregated into each cell body, and divided nuclei both located in one cell body.

embedded within the nuclear envelope (Peterson and Ris, 1976; Byers, 1981). Microtubules extend from both faces of the SPB into the nucleus and the cytoplasm. The SPB duplicates near the time of bud emergence. Separation of the SPBs allows the creation of a short bipolar spindle (~2 μm in diploid yeast cells) composed of kinetochore and polar microtubules. At anaphase, this spindle elongates until it stretches from one end of a large-budded cell to the other (~8–10 μm). Spindle elongation is relatively rapid; wild-type cells containing intermediate length spindles are seldom observed. Cytoplasmic microtubules extend from both spindle poles throughout mitosis.

To examine the effect of each conditional-lethal mutation on microtubule assembly in vivo, we shifted asynchronous cultures to their restrictive temperatures for two generation times, fixed the cells, and visualized microtubules by immunofluorescence. Cells with large buds and an undivided nucleus were considered to be arrested and scored for microtubule morphologies. In wild-type populations, only ~1% of the cells fit this category. For the tighter *tub2* alleles, most cells in the population were arrested and scored. For the leakier alleles, a smaller fraction of the cells appeared arrested and were scored. Quantitative analysis of mutant cultures is presented in Figure 6. Representative cells are shown in Figure 7.

Four of the mutants (*tub2-412*, *tub2-434*, *tub2-445*, and *tub2-551*) display similar microtubule arrays (Figure 7A). In these cells, microtubules appear to originate from a single point that is coincident with the DAPI-staining

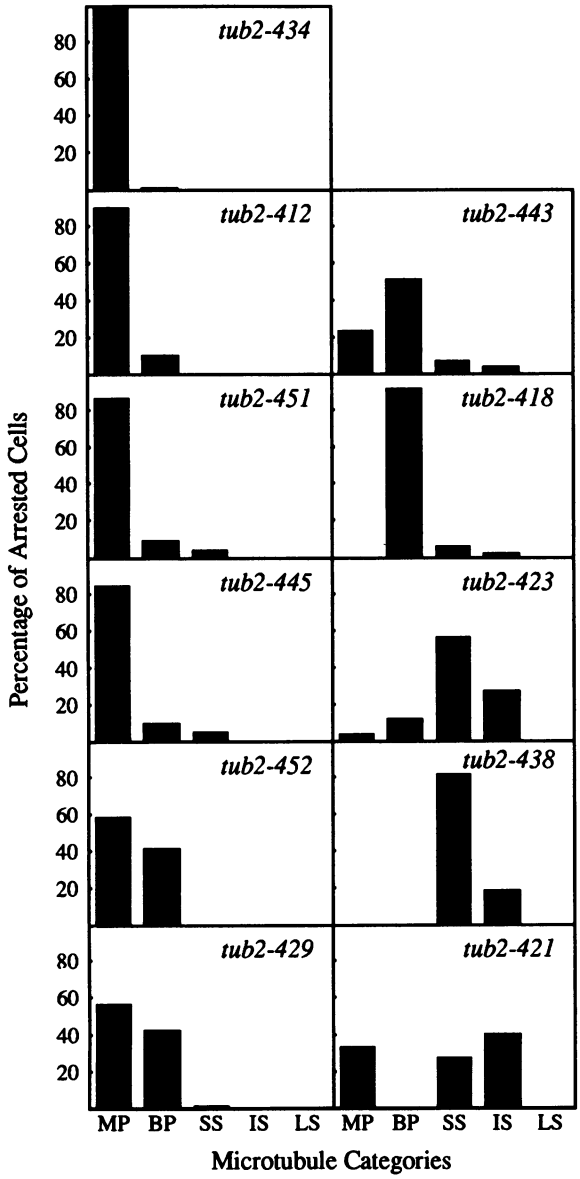

Figure 6. Quantitation of microtubule arrays in conditional-lethal mutant cells. Diploid cells homozygous for the indicated *tub2* allele were grown at 30°C and shifted to their restrictive temperature for two generation times. Microtubules were visualized by immunofluorescence. Microtubule arrays were scored only in those cells that possessed a large bud and an undivided nucleus (arrested cells). Categories are described in text. MP, monopolar array; BP, bipolar array; SS, short spindle; IS, intermediate spindle; LS, long spindle.

region. Usually one or two distinct bundles of microtubules extend into each cell body. It is not possible to be certain whether any particular bundle resides within the nucleus or the cytoplasm. However, two pieces of evidence lead us to believe that these are cytoplasmic microtubules. First, the intensity of staining is similar to that of wild-type cytoplasmic microtubules that is considerably less than spindle staining. Second, their orientation is as expected for cytoplasmic microtubules; they extend away from the DAPI-staining region toward the cell boundaries. We refer to these as "monopolar" microtubule arrays.

In most *tub2-418*–arrested cells, microtubules originate from two adjacent points that are coincident with the DAPI staining and extend into both cell bodies (Figure 7C). The two points of microtubule origin stain brightly and often appear as two side-by-side dots with a clear gap between them. We assume that these two points represent microtubules emanating from two separated SPBs. The staining intensity of the dots is similar to that of a wild-type spindle, suggesting that the dots represent short nuclear microtubules. However, the double-dot structure appears distinct from a normal short spindle that stains more evenly along its length. In addition, the distance between the dots is often less than the length of a short spindle. The long fibers extending from these dots into the cell bodies possess the staining intensity and orientation of cytoplasmic microtubules. We refer to these structures as "bipolar" microtubule arrays.

Three mutants (*tub2-429*, *tub2-443*, and *tub2-452*) have both monopolar and bipolar arrays. In about one-half of the *tub2-429* and *tub2-452* cells, microtubules appear to originate from a single point; in the other half, microtubules originate from two adjacent points (Figure 7E). *tub2-443* cells also contain monopolar and bipolar arrays. However, *tub2-443* cells differ substantially from *tub2-429* and *tub2-452* cells. All *tub2-443* cells contain extremely long cytoplasmic microtubules that often extend into the bud and wind back into the mother cell (Figure 7G). In addition, ~15% of the arrested cells contain two distinct and well-separated microtubule arrays.

Most *tub2-423* cells (~60%) contain short spindles that are indistinguishable from the wild-type short spindle (Figure 7I). These normal-looking spindles differ from the bipolar arrays described above; the spindle is generally longer and staining is even throughout its length. The *tub2-423* mutants also possess prominent cytoplasmic microtubules extending into both cell bodies. In addition, ~30% of these cells contain spindles that are clearly longer than the normal wild-type short spindle, often about twice as long (Figure 7I). We refer to these as "intermediate spindles." Fully elongated spindles are rare in this mutant.

The *tub2-421* and *tub2-438* mutations produce a weak cell cycle arrest. Only 34% of the *tub2-438* cells and 22% of *tub2-421* cells appear to be arrested by the criteria described above. Most *tub2-438*–arrested cells contain a short spindle indicating that this mutation may delay the onset of anaphase. The *tub2-421* arrested cells contain monopolar arrays and short and intermediate length spindles. These cells also contain an extensive and disorganized arrangement of cytoplasmic microtubules (Figure 7K).

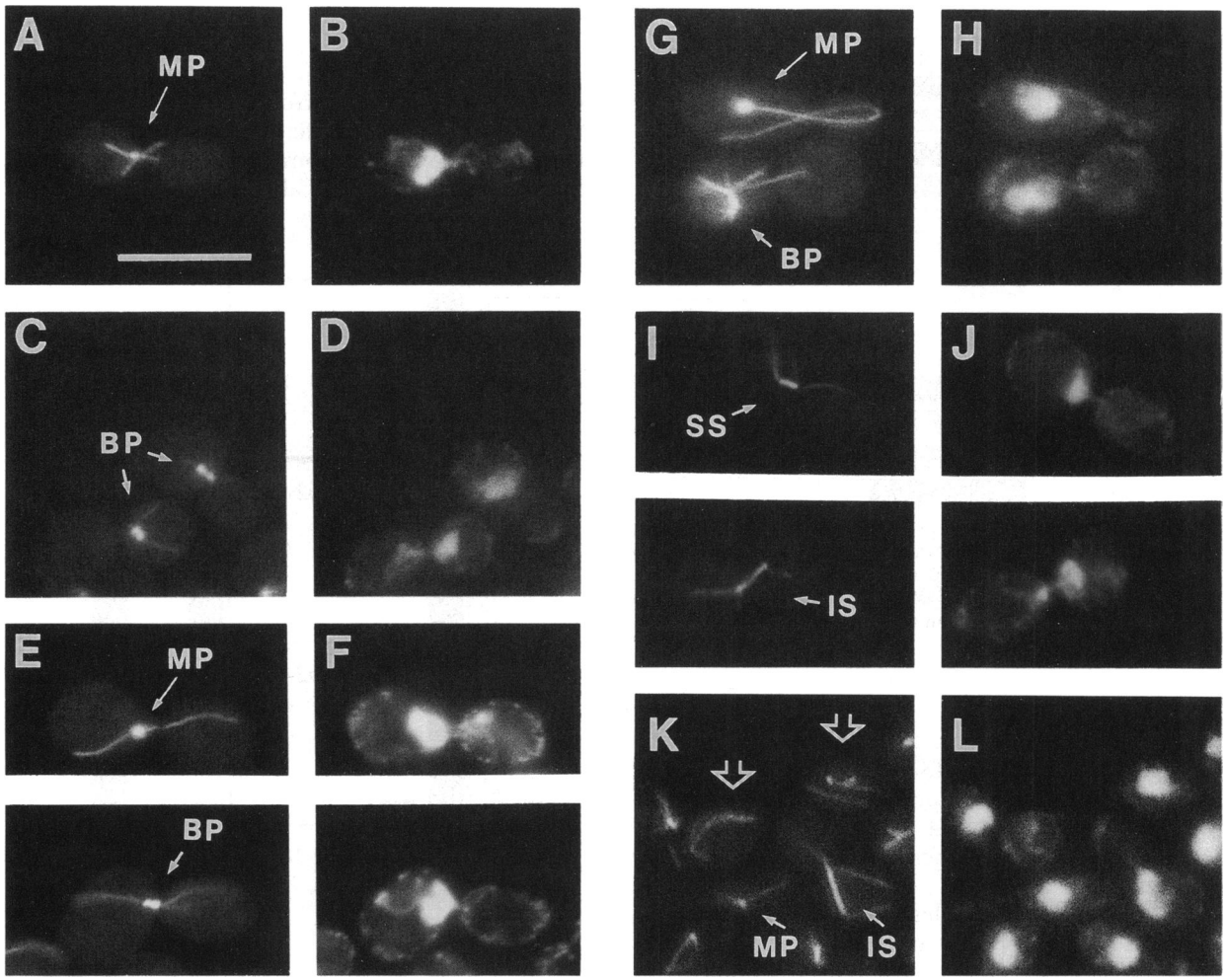

Figure 7. Fluorescence staining of conditional-lethal *tub2* mutant cells. Diploid cells homozygous for the indicated *tub2* allele were grown at 30°C and shifted to their restrictive temperature for two generation times. (A, C, E, G, I, and K) Microtubule immunofluorescence using tubulin-specific antibody. (B, D, F, H, J, and L) DAPI staining of cellular DNA. (A and B) *tub2-451;* (C and D) *tub2-418;* (E and F) *tub2-452;* (G and H) *tub2-443;* (I and J) *tub2-423;* (K and L) *tub2-421.* MP, monopolar array; BP, bipolar array; SS, short spindle; IS, intermediate spindle; open arrow, unorganized cytoplasmic microtubule arrays. Bar, 10 μm.

Phenotypic Characterization of Recessive-Lethal Mutants

A mutation that renders β-tubulin completely nonfunctional would cause recessive-lethality. In this case, we would expect the mutation to behave exactly like the deletion allele, *tub2-Δ1*. Alternatively, a recessive-lethal allele may produce a protein that is partially functional but unable to sustain cell growth as the sole β-tubulin protein in the cell. Several lines of evidence indicate that most of the recessive-lethal alleles retain partial function.

Many of the recessive-lethal mutations, when present in heterozygous diploids, alter the benomyl sensitivity of cells (Figure 8). Wild-type diploids are slightly more sensitive to benomyl than haploids; growth of diploids on 20 μg/ml is inhibited to some extent. A heterozygous diploid containing only one copy of *TUB2* (*TUB2/tub2-Δ1*) is even more sensitive; it grows only weakly on 20 μg/ml benomyl and even growth on 10 μg/ml is slowed. Heterozygous diploids containing three of the recessive-lethal alleles (*tub2-415, tub2-448,* and *tub2-455*) are indistinguishable from the *TUB2/tub2-Δ1* cells on benomyl. All of the others confer altered sensitivity to benomyl. The most extreme cases are the *TUB2/tub2-409* cells that grow on 80 μg/ml benomyl and the *TUB2/tub2-424* and *TUB2/tub2-437* cells that fail to grow or grow poorly on 5 μg/ml.

When the heterozygous diploid *TUB2/tub2-Δ1* (CUY409) is sporulated and the tetrads dissected, the *tub2-Δ1* spores germinate but arrest growth as a single cell with a large bud. Three of the recessive-lethal mutants behave similarly (*tub2-427, tub2-448,* and *tub2-*

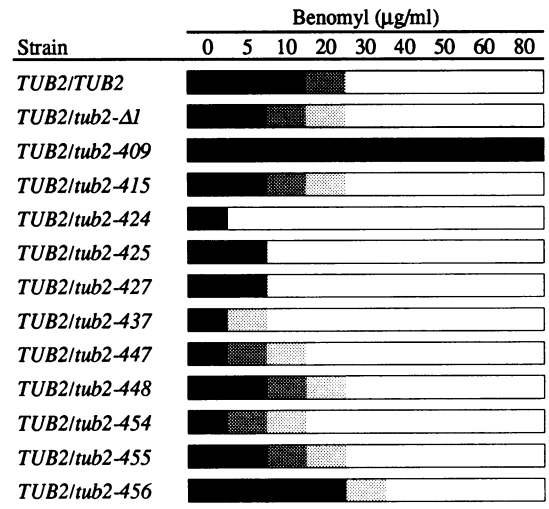

Figure 8. Growth on benomyl of heterozygous diploids containing wild-type and recessive-lethal *tub2* mutations. Growth on YPD plus benomyl was scored at 30°C and is relative to growth of the wild-type diploid on YPD without benomyl. Growth is proportional to stippling: heavy stippling > medium stippling > light stippling > no stippling = no growth.

456). Other mutants undergo one round of cell division to produce two cells (*tub2-437* and *tub2-447*) or a few rounds to produce microcolonies with four to six cells (*tub2-409, tub2-415, tub2-424, tub2-454,* and *tub2-455*). (We did not determine the microcolony size for the *tub2-425* mutant.)

To examine the microtubules in these growth-arrested cells, heterozygous diploids were sporulated. The spores were then isolated and incubated at 30°C. It took about 7 h for wild-type spores to germinate and complete one cell cycle. After this time, cells were fixed and microtubules visualized by immunofluorescence. One-half of the spores from each heterozygous diploid contain the recessive-lethal *tub2* allele; the other half are wild-type. In each case, 40–50% of the cells possess buds that are as large as the mother cell, indicating a cell cycle arrest. For each mutant, >80% of the large-bud–arrested cells contain a single undivided DAPI-staining region, indicating that chromosome segregation is blocked. We assumed that these cells carry the *tub2* mutation and scored them for their microtubule content. Quantitative analysis of each mutant culture is presented in Figure 9. Representative cells are shown in Figure 10.

Ninety-five percent of *tub2-Δ1* cells contain no detectable microtubules. Thus, the amount of wild-type tubulin carried over from the parent diploid is less than that needed to form any visible microtubules. Three mutants (*tub2-427, tub2-437,* and *tub2-448*) resemble *tub2-Δ1* cells; >80% of these cells lack all microtubule structures (Figure 10A). Three other mutants (*tub2-415, tub2-425,* and *tub2-447*) display a combination of three cell types. These cells contain either no staining, a dot of staining, or a single faint fiber. The dot presumably indicates very short microtubules extending from the SPB. The faint fiber usually appeared to be cytoplasmic because it headed away from the DAPI-staining region. We placed these latter cells into the monopolar category. However, they differ from the monopolar conditional-lethal mutants described above and the recessive-lethal

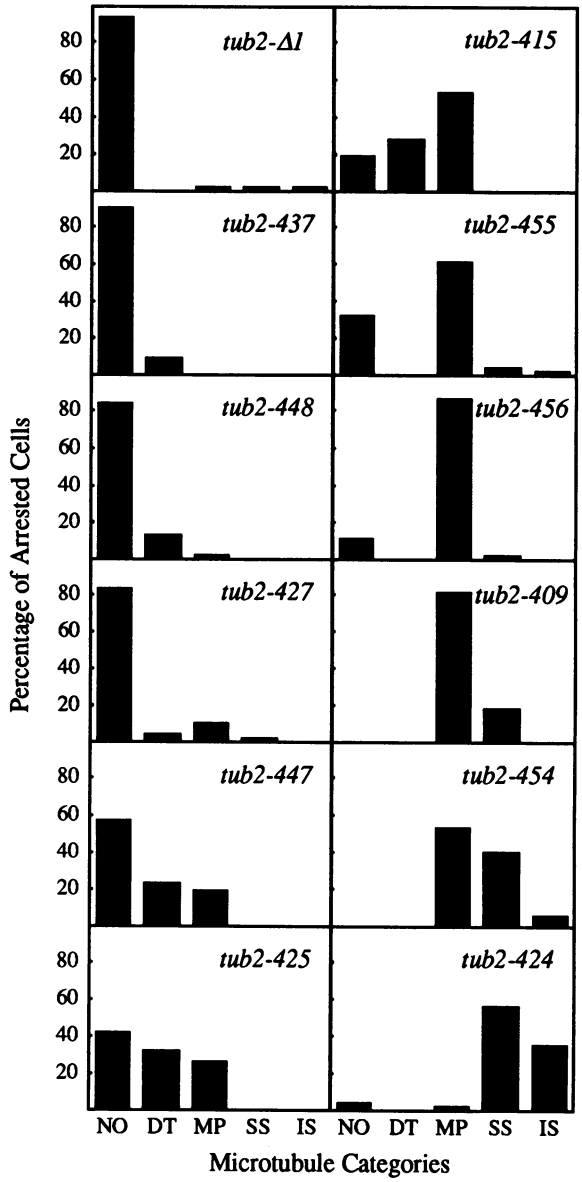

Figure 9. Quantitation of microtubule arrays in recessive-lethal mutant cells. Diploid cells heterozygous for the indicated *tub2* allele were sporulated, and the spores germinated at 30°C. Those haploid cells that displayed a cell cycle arrest were assumed to contain the mutant allele and scored. Microtubules were visualized by immunofluorescence. Categories are described in the text. NO, no microtubules; DT, dot of staining; MP, monopolar array; SS, short spindle; IS, intermediate spindle.

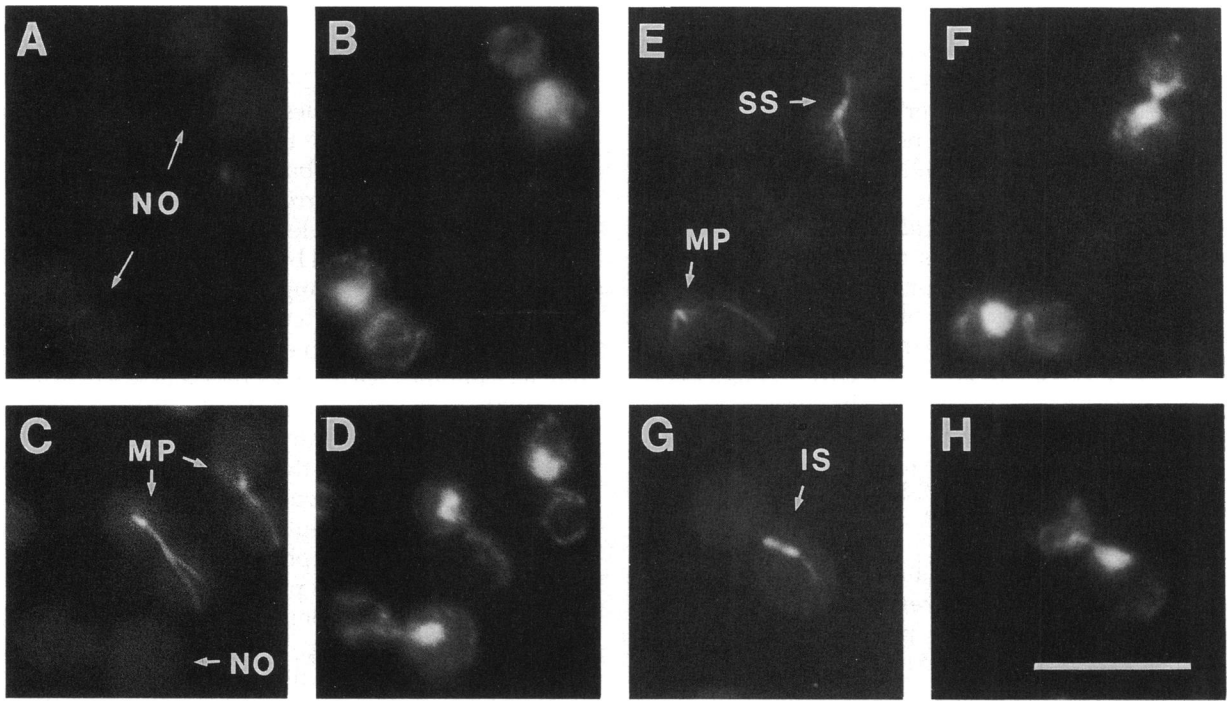

Figure 10. Fluorescence staining of recessive-lethal *tub2* mutant cells. Diploid cells heterozygous for the indicated *tub2* allele were sporulated, and the spores germinated at 30°C. Those haploid cells that displayed a cell cycle arrest were assumed to contain the mutant allele. (A, C, E, and G) Microtubule immunofluorescence using tubulin-specific antibody. (B, D, F, and H) DAPI staining of cellular DNA. (A and B) *tub2-448;* (C and D) *tub2-455;* (E and F) *tub2-454;* (G and H) *tub2-424.* NO, no microtubules; MP, monopolar array; SS, short spindle; IS, intermediate spindle. Bar, 10 μm.

mutants described below because they generally contain only a single fiber that stains much weaker than cytoplasmic microtubules in wild-type cells.

In most *tub2-409, tub2-455,* and *tub2-456* cells, one or two distinct bundles of microtubules extend from a single point (Figure 10C). The microtubules stain with about the same intensity as cytoplasmic microtubules in wild-type cells. These structures closely resemble the monopolar arrays of the conditional-lethal mutants described above.

In only two mutants (*tub2-424* and *tub2-454*) are a substantial number of bipolar spindles observed. About one-half of the *tub2-454* cells contain monopolar arrays, and half contain a short spindle similar to the wild-type metaphase spindle (Figure 10E). In contrast, >90% of the *tub2-424* cells contain a bipolar spindle. About 60% of these resemble the typical short spindle; the remainder are significantly longer and have been placed into the intermediate spindle category (Figure 10G).

DISCUSSION

Alanine-scanning Mutations

We have used a systematic approach to mutagenize the yeast gene encoding β-tubulin. This approach targets clusters of charged residues maximizing alterations on the protein surface and minimizing alterations in the protein interior. Wild-type residues are substituted with alanine that, in effect, simply truncates the charged amino acid's side chain; this alteration is unlikely to cause any long-range conformational change in the protein. Thus, the collection should be biased toward mutations whose primary effect is the removal of a charged patch from a single small domain on the surface of the protein. In this sense, these mutations are better defined than the random amino acid substitutions that make up the previous *tub2* alleles. Because the alanine-scanning mutations span the length of the amino acid sequence, it is likely that we have sampled much of the protein's surface in this study.

Importantly, this systematic process makes no assumptions about putative functional sites. An alternative to a systematic approach would be to target putative functional sites for mutation. However, the structure of β-tubulin has not been solved, and the assignment of functional regions of the protein is inexact. Furthermore, even in the case of an extensively characterized protein, it is difficult to predict which mutations will lead to genetically useful phenotypes. The unpredictability of mutant phenotypes is illustrated by the *tub2* alleles that contain overlapping sets of mutations.

1) *tub2-445* (K324A, E325A) cells are Cs but not Ts. We split these mutations to create *tub2-443* (K324A) and *tub2-444* (E325A). *tub2-443* cells are Ts but not Cs; *tub2-444* cells are neither Ts nor Cs. However, all three alleles confer modest super-sensitivity to benomyl.

2) Both *tub2-413* (D67A, E69A) and *tub2-416* (D74A, R77A) cells display wild-type growth. The *tub2-414* (D67A, E69A, G71W) and *tub2-415* (G71W, D74A, R77A) alleles are the same as the *tub2-413* and *tub2-416* alleles, respectively, except for the addition of the G71W mutation. The addition of G71W to D67A, E69A has no effect; *tub2-414* cells also show wild-type growth. However, addition of G71W to D74A, R77A has a major effect; the *tub2-415* allele is a recessive-lethal.

3) The *tub2-425* (K154A, R156A) allele is a recessive-lethal; the *tub2-423* (I152F, K154A, R156A) allele confers a Cs phenotype. Thus, the I152F mutation suppresses the lethality of K154A, R156A at 30°C.

Two of the previously isolated *tub2* alleles contain mutations in locations that overlap with alanine-scanning alleles. In one case, the phenotypes are similar. *tub2-405* (R391T) and *tub2-451* (K390A, K392A) cells are both Cs and supersensitive to benomyl. In the other case, they differ. *tub2-402* (R318W) cells are Cs, but *tub2-442* (R318A, K320A) cells are not. However, both mutations confer high levels of resistance to benomyl.

Conditional-Lethal Alleles

Alanine-scanning mutagenesis was very successful in generating conditional-lethal alleles that are most amenable to genetic analysis. Eleven of the 55 mutations conferred a Ts or Cs phenotype. In contrast, extensive random mutagenesis of this gene produced only five Cs and no Ts alleles (Huffaker *et al.*, 1988). Most of the new mutations display phenotypes that were not represented in the original collection. Thus, systematic mutagenesis has revealed a number of additional functional domains in β-tubulin. The conditional alleles reported here are not clustered but are rather evenly spread throughout the charged regions of the protein sequence.

Microtubules are known to perform two functions during the yeast mitotic cell cycle. Cytoplasmic microtubules are required to move the nucleus to the bud neck, and microtubules within the nucleus form the mitotic spindle that is responsible for nuclear division. Curiously, all but one of the conditional-lethal alanine-scanning mutations appear to affect primarily nuclear microtubule function; cytoplasmic microtubule function is relatively unaffected. This observation is consistent with the microtubule arrays that are present in these cells. All of the mutants possess prominent cytoplasmic microtubules. Only in the *tub2-421* and *tub2-443* cells do these appear unusual, being excessively long and often unorganized. On the other hand, many of the cells lack or assemble what appear to be aberrant spindle structures.

In four mutants (*tub2-412*, *tub2-434*, *tub2-445*, and *tub2-451*) all microtubules appear to originate from a single point. We refer to these as monopolar arrays. A single point of microtubule origin indicates that SPB separation has not occurred or that separated SPBs are very closely apposed. A less likely interpretation is that the SPBs have separated but only one is able to nucleate microtubules. The staining intensity and orientation of the fibers are typical of cytoplasmic microtubules. Although we are unable to state with certainty that all of the microtubules we observe reside in the cytoplasm, it seems likely that these cells lack all or most nuclear microtubules. The mutants appear to be the converse of the *tub2-401* mutant that, at one restrictive temperature, assembles a functional spindle but lacks cytoplasmic microtubules (Sullivan and Huffaker, 1992).

A second microtubule phenotype is displayed by *tub2-418*. These cells contain prominent cytoplasmic microtubules that extend from two closely apposed bright dots of tubulin staining. We refer to these as bipolar arrays. The two points of microtubule origin indicate that SPB separation has occurred. We speculate that these brightly staining microtubules reside in the nucleus because their intensity is similar to that of normal spindles that stain much more brightly than cytoplasmic microtubule bundles. However, these microtubules do not appear to form a normal bipolar spindle. First, wild-type spindles generally stain evenly along their length; these bipolar arrays stain brightly at their ends but weakly in the middle. Second, the distance between the two points is often, but not always, less than the length of a normal spindle. Thus, *tub2-418* cells appear to assemble an abnormal nuclear structure that is incapable of segregating chromosomes.

Three mutants (*tub2-429*, *tub2-443*, and *tub2-452*) arrest with both monopolar and bipolar arrays. It is possible that the distinction between these classes is more perceived than real. Distinguishing one bright staining region from two adjacent bright staining regions can be difficult at the level of immunofluorescence. The structures in these cells may be sufficiently different from those in *tub2-418* cells to make this distinction less certain. It is also possible that these mutants generate two different arrest phenotypes. This is not unexpected when asynchronous cultures are shifted to a restrictive temperature. Cells that encounter the temperature block at one stage of the cell cycle may display a different terminal arrest from those that encounter the block at a different stage of the cell cycle. This has been shown to be the case for nocodazole-arrested cells (Jacobs *et al.*, 1988). Nocodazole treatment will block SPB separation. However, cells that are exposed to nocodazole after they have completed SPB separation will arrest with two separated but closely apposed SPBs.

Most *tub2-423* and *tub2-438* cells contain a short bipolar spindle and prominent cytoplasmic microtubules that are indistinguishable from wild-type metaphase microtubule arrays. The fact that these cells do not undergo spindle elongation suggests that they have some defect in spindle assembly that is not detectable by immunofluorescence. About 30% of the *tub2-423* cells contain spindles that are clearly longer. These could be aberrant metaphase spindles or spindles that have begun but are unable to complete anaphase elongation.

Interestingly, most of the conditional-lethal mutations appear to have a major effect on nuclear microtubule assembly and little, if any, on cytoplasmic microtubule assembly. There are several potential explanations for a specific effect on nuclear microtubule assembly. One possibility is that a mutation makes polymerization of tubulin subunits intrinsically more cold or heat sensitive. Because yeast contain only one β-tubulin, both nuclear and cytoplasmic microtubules must be altered. However, the environment within the nucleus may be less favorable for tubulin polymerization making nuclear microtubules more sensitive to mutations that affect microtubule assembly. A severe defect of this nature could lead to a complete lack of nuclear microtubules. A more moderate defect might limit the assembly of some spindle structures. Alternatively, a mutation may not modify the intrinsic polymerization properties of tubulin, but instead, block a particular microtubule-protein interaction. This interaction could be critical for some aspect of spindle assembly but not required for cytoplasmic microtubule assembly. A third explanation depends on the fact that the yeast nuclear envelope remains intact throughout the cell cycle. This means that yeast cells must have some mechanism for transporting tubulin subunits into the nucleus. A β-tubulin mutation may interfere with the ability of tubulin subunits to interact with the transport apparatus and diminish the ability of cells to carry tubulin into the nucleus. Again, a severe defect in transport would eliminate all nuclear microtubules; a more modest defect might allow assembly of some spindle structures.

Lethal Alleles

The site-directed mutagenesis protocol used to construct the alanine-scanning mutants allowed us to recover recessive-lethal alleles in heterozygous diploids. These mutations could not be easily obtained by random mutagenesis and screening. The strong conservation of the β-tubulin sequence in evolution suggested that it might be difficult to make viable mutations in *TUB2*. However, only 14 of the 55 mutations we constructed (12 of the 49 that were strictly charged to alanine mutations) are lethal. Three of these are dominant and 11 are recessive. The lethal alleles identify a subset of the β-tubulin sequence that is most sensitive to amino acid alterations and presumably most critical for β-tubulin function. All but three of the lethal substitutions are located in three regions of the proteins.

1) Five lethal substitutions (*tub2-453* through *tub2-457*) cluster near the C-terminus of the protein between amino acid residues 405 and 432. The adjacent *tub2-451* and *tub2-452* alleles are conditionally lethal, and *tub2-452* cells grow slowly even at permissive temperatures. Thus, this stretch of amino acids is highly sensitive to alterations.

2) Three lethal substitutions (*tub2-446* through *tub2-448*) cluster within amino acid residues 327–343. Two (*tub2-443* and *tub2-445*) of the three mutations directly adjacent to this cluster are conditionally lethal.

3) Three recessive-lethal substitutions (*tub2-424*, *tub2-425*, and *tub2-427*) sit between residues 152–158. These mutations are close to the sequence GGGTGSG at residues 140–146. This latter sequence is highly conserved in α-, β-, and γ-tubulins and is found in the *Escherichia coli* GTP-binding protein FtsZ (de Boer *et al.*, 1992; RayChuadhuri and Park, 1992). It is a variation of the GTP/GDP binding motif of the GTPase superfamily of proteins. This region of β-tubulin is postulated to be the phosphate-binding loop on the basis of its similarity to the nucleotide-binding folds of adenylate kinase, dehydrogenases, and flavodoxins (Krauhs *et al.*, 1981).

4) One of the remaining three recessive-lethal alleles, *tub2-409*, overlaps the 28–38 residue region of β-tubulin that has been proposed to lie in a zone of interaction between tubulin dimers in assembled microtubules (Chene *et al.*, 1992). This allele also confers extreme resistance to benomyl in heterozygous diploid cells.

Any mutation that renders β-tubulin completely nonfunctional would be recessive-lethal and behave exactly like the deletion allele *tub2-Δ1*. The *tub2-Δ1* allele confers three distinctive phenotypes. *tub2-Δ1/TUB2* heterozygous diploids are slightly more sensitive to benomyl than wild-type diploids. Haploid *tub2-Δ1* spores germinate but arrest as single large-budded cells. The large-budded cells produced after germination of *tub2-Δ1* spores lack detectable microtubules.

The *tub2-448* phenotype is nearly identical to that of *tub2-Δ1* so it may also be a null allele. The *tub2-427* and *tub2-437* alleles confer phenotypes that are similar but not identical to the *tub2-Δ1* allele. After spore germination, both produce large-budded cells that lack detectable microtubules. However, most of the germinated *tub2-437* spores manage to complete one cell cycle indicating that they possess some microtubules; these may exist only transiently or be too frail to detect by immunofluorescence. In addition, *tub2-427/TUB2* and *tub2-437/TUB2* cells are more sensitive to benomyl than *tub2-Δ1/TUB2* cells. Three recessive-lethal mutants (*tub2-415*, *tub2-425*, and *tub2-447*) contain detectable microtubules indicating that β-tubulin produced in these cells retains partial function; however, these mutants

are clearly deficient in microtubule assembly in vivo. Five other recessive-lethal alleles (*tub2-409*, *tub2-424*, *tub2-454*, *tub2-455*, and *tub2-456*) differ significantly from the *tub2-Δ1* allele. Germinated spores containing these mutations produce microcolonies with 4–6 cells (except *tub2-456* cells), and these cells contain substantial microtubule arrays. Although *tub2-409*, *tub2-455*, and *tub2-456* cells do not assemble bipolar spindles, about one-half of the *tub2-454* cells and virtually all of the *tub2-424* cells contain these structures. The *tub2-409/TUB2* and *tub2-424/TUB2* heterozygous diploids also display dramatic differences in benomyl sensitivity.

We were unable to obtain yeast cells containing three of the mutations and infer that these alterations cause dominant lethality. By definition, these alleles have gained some function that is deleterious to cells. For example, dimers containing the mutant β-tubulin may add to growing polymers but block subsequent dimer addition. The phenotype of these alleles can be studied by expressing the mutant genes from a promoter that can be regulated.

Conclusion

Clustered charged-to-alanine scanning mutagenesis has allowed us to obtain an unbiased set of mutations that span the entire sequence of the yeast β-tubulin protein. The phenotypic diversity within this collection suggests that many of the mutants will be useful in dissecting spindle assembly and function, identifying associated cellular components, and relating the biochemical properties tubulin proteins to their function in vivo.

ACKNOWLEDGMENTS

We thank David Botstein and Ken Wertman for helpful discussions and providing plasmid pKFW46 and Anthony Bretscher for critical reading of the manuscript. This work was supported by National Institutes of Health grant GM-40479 and a Cornell Biotechnology Program Predoctoral Fellowship to R.A.R.

REFERENCES

Barnes, G., Louie, K.A., and Botstein, D. (1992). Yeast proteins associated with microtubules in vitro and in vivo. Mol. Biol. Cell *3*, 29–47.

Bass, S.H., Mulkerrin, M.G., and Wells, J.A. (1991). A systematic mutational analysis of hormone-binding determinants in the human growth hormone receptor. Proc. Natl. Acad. Sci. USA *88*, 4498–4502.

Becker, D.M., and Guarente, L. (1991). High-efficiency transformation of yeast by electroporation. Methods Enzymol. *194*, 182–184.

Bennett, W.F., Paoni, N.F., Keyt, B.A., Botstein, D., Jones, A.J.S., Presta, L., Wurm, F.M., and Zoller, M.J. (1991). High resolution analysis of functional determinants on human tissue-type plasminogen activator. J. Biol. Chem. *266*, 5191–5201.

Bond, J.F., Fridovich, K.J.L., Pillus, L., Mulligan, R.C., and Solomon, F. (1986). A chicken-yeast chimeric beta tubulin protein is incorporated into mouse microtubules in-vivo. Cell *44*, 461–468.

Byers, B. (1981). Cytology of the yeast life cycle. In: The Molecular Biology of the Yeast *Saccharomyces*, ed. J.N. Strathern, E.W. Jones, and J.R. Broach, Cold Spring Harbor, NY: Cold Spring Harbor Laboratory Press, 59–96.

Chene, P., Mazarguil, H., and Wright, M. (1992). Microtubule assembly protects the region 28-38 of the β-tubulin subunit. Cell Motil. Cytoskeleton *22*, 25–37.

de Boer, P., Crossley, R., and Rothfield, L. (1992). The essential bacterial cell-division protein FtsZ is a GTPase. Nature *359*, 254–256.

Delgado, M.A., and Conde, J. (1984). Benomyl prevents nuclear fusion in *Saccharomyces cerevisiae*. Mol. & Gen. Genet. *193*, 188–189.

Gibbs, C.S., and Zoller, M.J. (1991). Rational scanning mutagenesis of a protein kinase identifies functional regions involved in catalysis and substrate interactions. J. Biol. Chem. *266*, 8923–8931.

Guthrie, C., and Abelson, J. (1982). Organization and expression of tRNA genes in *Saccharomyces cerevisiae*. In: The Molecular Biology of the Yeast *Saccharomyces*, ed. J.N. Strathern, E.W. Jones, and J.R. Broach, Cold Spring Harbor, NY: Cold Spring Harbor Laboratory Press, 487–528.

Huffaker, T.C., Thomas, J.H., and Botstein, D. (1988). Diverse effects of β-tubulin mutations on microtubule formation and function. J. Cell Biol. *106*, 1997–2010.

Jacobs, C.W., Adams, A.E.M., Szaniszlo, P.J., and Pringle, J.R. (1988). Functions of microtubules in the *Saccharomyces cerevisiae* cell cycle. J. Cell Biol. *107*, 1409–1426.

Kassir, Y., and Simchen, G. (1991). Monitoring meiosis and sporulation in *Saccharomyces cerevisiae*. Methods Enzymol. *194*, 94–109.

Kilmartin, J.V. (1981). Purification of yeast tubulin by self-assembly in vitro. Biochemistry *20*, 3629–3633.

Kilmartin, J.V., and Adams, A.E.M. (1984). Structural rearrangements of tubulin and actin during the cell cycle of the yeast *Saccharomyces*. J. Cell Biol. *98*, 922–933.

Krauhs, E., Little, M., Kempf, T., Hofer-Warbinek, R., Ade, W., and Ponstingl, H. (1981). Complete amino acid sequence of β-tubulin from porcine brain. Proc. Natl. Acad. Sci. USA *78*, 4156–4160.

Matsuzaki, F., Matsumoto, S., and Yahara, I. (1988). Truncation of the carboxy-terminal domain of yeast b-tubulin causes temperature-sensitive growth and hypersensitivity to antimitotic drugs. J. Cell Biol. *107*, 1427–1435.

Neff, N.F., Thomas, J.H., Grisafi, P., and Botstein, D. (1983). Isolation of the β-tubulin gene from yeast and demonstration of its essential function in vivo. Cell *33*, 211–219.

Peterson, J.B., and Ris, H. (1976). Electron-microscopic study of the spindle and chromosome movement in the yeast, *Saccharomyces cerevisiae*. J. Cell Sci. *22*, 219–242.

Pillus, L., and Solomon, F. (1986). Components of microtubular structures in *Saccharomyces cerevisiae*. Proc. Natl. Acad. Sci. USA *83*, 2468–2472.

RayChuadhuri, D., and Park, J.T. (1992). *Escherichia coli* cell-division gene ftsZ encodes a novel GTP-binding protein. Nature *359*, 251–254.

Schatz, P., Solomon, F., and Botstein, D. (1988). Isolation and characterization of conditional-lethal mutations in the TUB1 α-tubulin gene of the yeast *Saccharomyces cerevisiae*. Genetics *120*, 681–695.

Sheen, J. (1991). High-efficiency transformation by electroporation. In: Current Protocols in Molecular Biology, ed. R.B.F.M. Ausubel, R.E. Kingston, D.D. Moore, J.G. Seidman, J.A. Smith, and K. Struhl, New York: John Wiley & Sons, 1.8.4–1.8.8.

Sherman, F. (1991). Getting started with yeast. Methods Enzymol. *194*, 3–21.

Sikorski, R.S., and Hieter, P. (1989). A system of shuttle vectors and yeast host strains designed for efficient manipulation of DNA in *Saccharomyces cerevisiae*. Genetics *122*, 19–27.

Stearns, T., and Botstein, D. (1988). Unlinked noncomplementation: isolation of new conditional-lethal mutations in each of the tubulin genes of *Saccharomyces cerevisiae*. Genetics *119*, 249–260.

Sullivan, D.S., and Huffaker, T.C. (1992). Astral microtubules are not required for anaphase B in *Saccharomyces cerevisiae*. J. Cell Biol. *119*, 379–388.

Thomas, J., Neff, N., and Botstein, D. (1985). Isolation and characterization of mutations in the β-tubulin gene of *Saccharomyces cerevisiae*. Genetics *112*, 715–734.

Treco, D.A., and Winston, F. (1991). Random spore analysis. In: Current Protocols in Molecular Biology, ed. R.B.F.M. Ausubel, R.E. Kingston, D.D. Moore, J.G. Seidman, J.A. Smith, and K. Struhl, New York: John Wiley & Sons, 13.2.10–13.2.12.

Wertman, K.F., Drubin, D.G., and Botstein, D. (1992). Systematic mutational analysis of the yeast ACT1 gene. Genetics *132*, 337–350.